African Journal of Applied Research
Vol. 5, No. 1 (2019), pp. 46-59
http://www.ajaronline.com
http://doi.org/10.26437/ajar.05.01.2019.04

DEVELOPMENT OF BIOMECHANICAL MODEL AND FEA MODAL ANALYSIS OF THE GRAVID HUMAN UTERUS EXPOSED TO RAMP-INDUCED VIBRATION

Akowuah, E.[1], Andoh, P. Y[2]. and Ampofo, J[3].

[1]*Mechanical and Manufacturing Engineering Department, School of Engineering, University of Energy and Natural Resources, Sunyani, Ghana.*
[2&3]*Mechanical Engineering Department, College of Engineering, Kwame Nkrumah University of Science and Technology, Kumasi, Ghana.*

[1]ericakowuah15@gmail.com
[2]andohp_2@yahoo.com
[3]josh.ampofo@gmail.com

ABSTRACT
Natural frequencies, frequencies at which bodies resonate and consequently fail, are very crucial in studying the dynamics of mechanical and biomechanical components. A number of researchers have carried out several studies on vehicle occupants with regard to various sitting postures, seat types and road roughness levels in which resonant frequencies of certain body parts have been established. In the area of vibration analysis for pregnant occupant, there is practically no significant research to pinpoint the frequencies at which the tummy of the pregnant woman could critically resonate. Therefore, this work is focused on developing a plausible biomechanical model and to determine the natural frequencies of the gravid human uterus. The Kelvin-Voigt's and Maxwell's spring-damper models were used to represent the amniotic fluid and ligaments of the uterus respectively. Finite element modal analysis was performed in ANSYS workbench (version 15.0) and the 3-dimensional model realized 300 modes at frequencies below 7.30 Hz. It is found that the gravid human uterus has a first principal resonance of 1.03 Hz and the second and third principal resonance occurred at 2.68 Hz and 3.99 Hz respectively. Interestingly, the foetus has a singleton principal resonance frequency of 1.03 Hz whilst the uterus wall has two principal frequencies of 3.05 Hz and 4.62 Hz. It is recommended that assessment of stresses and deformation on the gravid human uterus under ramp-induced vibration is crucial for future female reproductive health studies.
Keywords: Natural frequency, mode shape, deformation, foetus, ligament.

1.0 INTRODUCTION
Knowledge on the natural frequencies of living organs and non-living components are very crucial for comprehensive studies on the mechanical deformation and failure dynamics of such bodies. Naturally, a body is inefficient in functioning when performing a task at or near one of its natural frequencies. Just like a non-living mechanical component, which would resonate at one of its natural frequencies, living tissue and or organ also behave in a similar fashion and consequently its natural frequencies could also be estimated to avoid undesired resonance during

ISSN: 2408-7920

the normal physiological development and functioning. Living organs in the human body are susceptible to a number of vibrations - ranging from those emitted by home appliances to workplace and transport machineries, among others. Whilst vibrations could be used to correct some disease in the human body, vibrations levels beyond certain thresholds could also lead to psychomotor deficit which result in reduction in human alertness and induced drowsiness *(Azizan & Ittianuwat, 2016).*

Anatomically, the non-pregnant uterus is a pear-shaped hollow but thick-walled living organ hooked by five pairs of ligaments that support it centrally in the pelvic cavity. The average dimension of the non-pregnant uterus is 75 mm long by 50 mm wide by 30 mm thick *(Miftahof, 2011)* and has four parts, namely; the fundus, the body, uterotubal angles and the cervix. The ligaments are; cardinal, uterosacral, round, broad and ovarian ligaments. The morpho-structutral functional unit of the muscle tissue of the uterus is the uterine smooth muscle cell called myocyte *(Ackermann & Gauwerky, 2003).* The uterus is housed within the abdominal muscles and the pelvic floor. The pelvic bones are covered by a dome-shaped muscular sheet called levator ani *(Fritsch, Lienemann, Brenner & Ludwikowski, 2012)*. The gravid uterus undergoes significant dynamic changes in terms of location, size and structure to adjust itself to the needs of the growing embryo. The pregnant uterus grows and expands outward and upward from the pelvis and occupies the lower and middle abdomen with full term gestation average dimension of 410 mm long by 360 mm wide by 5.2 mm thick at 110 mm mean radius of curvature *(Sfakiani, Buhimschi, Pettker, Magliore, Turan, Hamer & Buhimschi, 2008; Celeste & Mercer, 2008).*

The amniotic fluid of human is obtained from the maternal plasma and foetal urine and is known to consist of organic and inorganic constituents *(Adama van Scheltema, In't Anker, Vereecken, Vandenbussche, Kanhai, & Devlieger, 2005; Underwood, Gilbert & Sherman, 2005).* The organic constituents include; creatinine, urea, glucose, and proteins whilst the inorganic constituents comprise electrolytes such as sodium, potassium, chloride and carbon dioxide *(Fischer, 2008).* According to Rosati, Pola, Riccardi, Flore, Tondi and Bellati (1991), the upper bound of foetus amniotic fluid viscosity is found to be 1.17 centiPoise.

Biological components are usually hyperplastic in nature and are modeled as viscoelastic materials, in which the elastic moduli vary with time. Several models exist for analyzing viscoelastic materials. Generally, viscoelastic media are modelled based on Kelvin-Voigt's model whilst viscous media are also modelled based on the Maxwell's model. The Kelvin-Voigt element is a parallel spring-damper arrangement and it could be used to approximate the stiffness level of viscoelastic media *(Chheliya, 2015)*. Similarly, viscoelastic liquids are best approximated by the Maxwell's element, having spring and damper elements in series *(Greco & Marano, 2015).*

In the area of natural frequency analysis, a number of researchers have over the years contributed significantly to how vibrations have had diverse impacts on the human body *(Conza & Rixen, 2006; Kim, Kim &Yoon, 2005; Rubin, 2002; Matsumoto & Griffin, 2001; Cho, & Yoon, 2001; Kitazaki & Griffin,1997).* For instance, it is known that the frequency range of 1-10 Hz is dangerous for humans and the internal organs *(Dariusz & Jaskiewicz, 2014).* However, a lot needs to be done in the area of organ-specific frequency analysis in fully exploring the biomechanical behaviour of organs under various vibrational impacts. Research into the natural deformation modes of organs are feasible, especially when analysis tools *(Stolarski, Nakasone &*

ISSN: 2408-7920

Yoshimoto, 2007; Petyt, 2005; Kent, 2005) and techniques *(Harris & Piersol, 2001; Lui & Li, 2013)* are readily available for such discourses.

Unfortunately, the numerical models and simulations done on pregnant women that are related to the gravid uterus have been centered on the estimation of the risk levels of the foetus and rapturing of the umbilical cord in road crashes only *(Klinich, Schneider, Eby, Rupp & Pearlman, 2004; Pearlman, 2000)* and no investigation has been done on the gravid human uterus under ramp-induced vibration (RIV). Consequently, there is a knowledge gap in respect of the range of resonance frequencies which could be detrimental to the uterus wall and foetus. Therefore, objectives of this study were to develop and validate a biomechanical model that is an analogous representative of the gravid human uterus. And to determine its natural frequencies under RIV excitations using FEA modal analysis tool (ANSYS Workbench).

2.0 MATERIALS AND METOD

Biomechanical Model of the Gravid Uterus

The gravid tummy accommodates the gravid uterus which is centrally positioned within the pelvis in the lower abdomen. Figure 1 represents an 11 DOF model of an ellipsoid-shaped gravid uterus treated as a bioshell with a suspended 5 DOF foetus under some assumptions. The assumptions on uterus tissues, liquor and foetus body that were used to enhance the theoretical analysis of the gravid uterus included the following**.** Gravid uterus wall was modeled as isotropic viscoelastic material whilst the liquor was modeled as a viscoelastic fluid having constant viscosity and density, within which a rigid foetus is suspended.

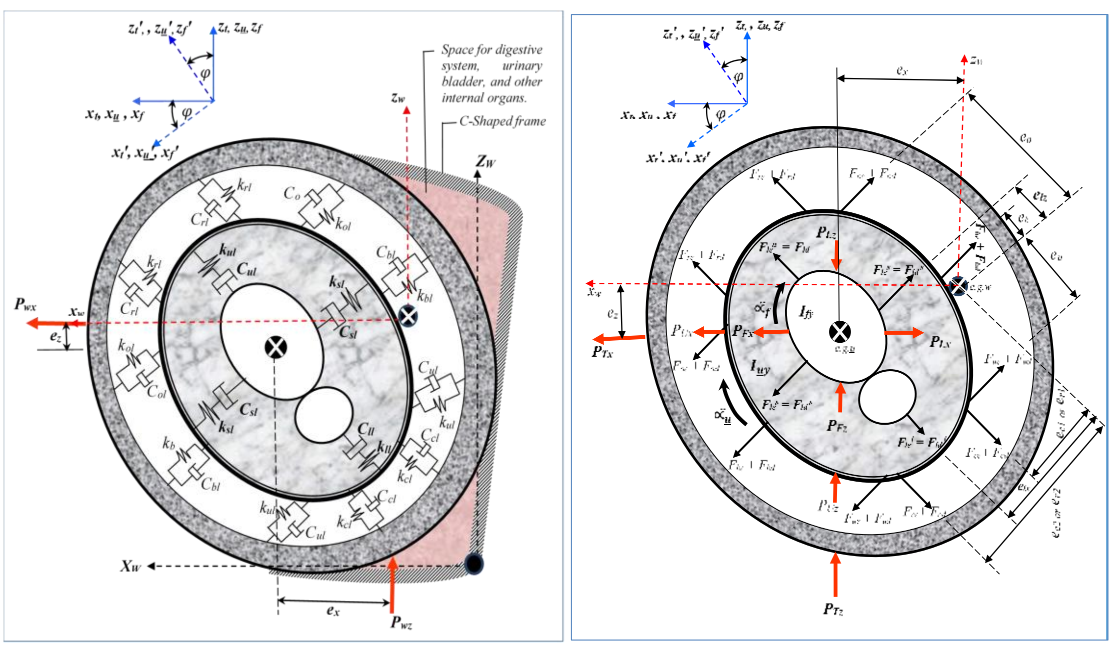

(a) (b)

Figure 1: Eleven DOF biomechanical model of the gravid uterus with 5 DOF two rigid body foetus (a) and free body diagram of the model (b).

African Journal of Applied Research
Vol. 5, No. 1 (2019), pp. 46-59
http://www.ajaronline.com
http://doi.org/10.26437/ajar.05.01.2019.04

The liquor was modelled as Maxwell's spring-damper in series connections. Uterus was assumed to be inclined within the spherical tummy at an anteflexion angle, φ to the z axis and held in place by the five (5) pairs of evenly spaced ligaments, namely; round, ovarian, broad, cardinal and uterosacral ligaments. And each ligament was also modelled as Kelvin-Voigt spring-damper in parallel connections. The developed linear and pitching vibratory motions for the foetus and uterus within the tummy compartments are given by Equations 1 through 9. The linear uterus equations in z and x directions are given by Equations 1 and 2.

$$m_{\underline{u}}\ddot{z}_{\underline{u}} + 2k_c(z_{\underline{u}} - z_t)cos\varphi + 2C_c(\dot{z}_{\underline{u}} - \dot{z}_t)cos\varphi - 2k_r(z_{\underline{u}} - z_t)cos\varphi - 2C_r(\dot{z}_{\underline{u}} - \dot{z}_t)cos\varphi = P_{Uz} \quad (1)$$

$$m_{\underline{u}}\ddot{x}_{\underline{u}} + 2k_c(x_{\underline{u}} - x_t)sin\varphi + 2C_c(\dot{x}_{\underline{u}} - \dot{x}_t)sin\varphi - 2k_r(x_{\underline{u}} - x_t)sin\varphi - 2C_r(\dot{x}_{\underline{u}} - \dot{x}_t)sin\varphi = P_{Ux} \quad (2)$$

Where P_{Uz} and P_{Ux} are the vertical and horizontal excitations of uterus in z and x direction respectively. And the terms associated with subscript $\underline{u}$ and t are related to uterus and tummy parameters. The five terms in the left-hand sides of Equations 1 and 2 are – from left to right; the inertial force of uterus, springing force in cardinal ligament, damping force in cardinal ligament, springing force in round ligament and damping force in round ligament along the vertical (z) and horizontal longitudinal (x) directions. The overall uterus pitching motion is given by Equation 3 and with Equation 4 as a set of substitutes for Equation 3. Where e_x and e_z are the horizontal and vertical eccentricities between c.g.w and c.g.u respectively. Whilst e_r and e_c are those associated with ligament elastic (e) and damping (d) forces; F_{ce}, F_{cd} *for cardinal ligament forces and* F_{re}, F_{rd} for round ligament forces.

$$I_{\underline{u}y}\ddot{\propto}_{\underline{u}} + (e_{r1} + e_{r2})(F_{re} + F_{rd}) - (e_{c1} + e_{c2})(F_{ce} + F_{cd}) = -(e_x P_{Uz} + e_z P_{Ux}) \quad (3)$$

$$\left.\begin{aligned} F_{ce} &= \sqrt{[k_c(z_{\underline{u}} - z_t)]^2 + [k_c(x_{\underline{u}} - x)]^2} \\ F_{re} &= \sqrt{[k_r(z_{\underline{u}} - z_t)]^2 + [k_r(x_{\underline{u}} - x)]^2} \\ F_{cd} &= \sqrt{[C_c(\dot{z}_{\underline{u}} - \dot{z}_t)]^2 + [C_c(\dot{x}_{\underline{u}} - \dot{x}_t)]^2} \\ F_{rd} &= \sqrt{[C_r(\dot{z}_{\underline{u}} - \dot{z}_t)]^2 + [C_r(\dot{x}_{\underline{u}} - \dot{x}_t)]^2} \end{aligned}\right\} \quad (4)$$

And the four terms in Equation 3 are – from left to right; torque due to uterus moment of inertia, torque due to round ligament, torque due to cardinal ligament and sum of base excitation torques on uterus. The effective linear motion of foetus in cephalic presentation are given by Equations 5 and 6 for z and x directions respectively. Where the terms associated with *f* are related to foetus parameters and the forces associated with superscript *u* (upper), and *l* (lower) are linked to elastic (e) and damping (d) forces; F_{le}, F_{ld} of liquor forces acting above and below of foetus. Equation 7 is the set of substitutes used in Equations 5 and 6. The four terms in Equations 5 and 6 are – from left to right; combined foetus inertial force and added mass force, lower liquor force, upper liquor force and base excitation force on foetus for the z and x directions respectively.

ISSN: 2408-7920

$$(m_f + K_o M)\ddot{z}_f - (F^l_{le} + F^l_{ld}) + (F^u_{le} + F^u_{ld}) = P_{FZ} \quad (5)$$

$$(m_f + K_o M)\ddot{x}_f - (F^l_{le} + F^l_{ld}) + (F^u_{le} + F^u_{ld}) = P_{Fx} \quad (6)$$

$$\left.\begin{aligned} F^l_{le} &= k^l_l(z_f - z_{\underline{u}}) = k^l_l(x_f - x_{\underline{u}}) \\ F^u_{le} &= k^u_l(z_f - z_{\underline{u}}) = k^u_l(x_f - x_{\underline{u}}) \\ F^l_{ld} &= C^l_l(\dot{z}_f - \dot{z}_{\underline{u}}) = C^l_l(\dot{x}_f - \dot{x}_{\underline{u}}) \\ F^u_{ld} &= C^u_l(\dot{z}_f - \dot{z}_{\underline{u}}) = C^u_l(\dot{x}_f - \dot{x}_{\underline{u}}) \end{aligned}\right\} \quad (7)$$

Equation 8 also gives foetus pitching motion in the cephalic presentation. Where e_{lz} represents the eccentricity associated with liquor forces and *M* is the mass of liquor opposing the foetus motion. Equation 9 is the set of substitutes used in Equation 8. The three terms in Equation 8 represent – from left to right; the combined torque on foetus due to inertia and added mass force, torque due to liquor forces and base excitation forces.

$$[I_{fy} \ddot{\alpha}_f + K_o M(\ddot{x}_f e_z + \ddot{z}_f e_x)] + e_{lz}(F^u_{le} + F^u_{ld} - F^l_{le} - F^l_{ld}) = e_x P_{Fz} + e_z P_{Fx} \quad (8)$$

$$\left.\begin{aligned} F^u_{le} &= \sqrt{[k^u_l(x_f - x_{\underline{u}})]^2 + [k^u_l(z_f - z_{\underline{u}})]^2} \\ F^u_{ld} &= \sqrt{[C^u_l(\dot{x}_f - \dot{x}_{\underline{u}})]^2 + [C^u_l(\dot{z}_f - \dot{z}_{\underline{u}})]^2} \\ F^l_{le} &= \sqrt{[k^l_l(x_f - x_{\underline{u}})]^2 + [k^l_l(z_f - z_{\underline{u}})]^2} \\ F^l_{ld} &= \sqrt{[C^l_l(\dot{x}_f - \dot{x}_{\underline{u}})]^2 + [C^l_l(\dot{z}_f - \dot{z}_{\underline{u}})]^2} \end{aligned}\right\} \quad (9)$$

Geometric Construction of the Gravid Human Uterus

In order to numerically model the gravid uterus for fatigue stress simulation, a plausible geometric shape of the gravid uterus was a key requirement. Based on the descriptions given by Miftahof and Nam (2011) and the concept of 'open-belt drive arrangement' in tandem with the theory of tangency, the gravid uterus profile equation was deduced. Equation 10 and sub-equations 11 and 12 were the analytical equations obtained from the analytical gravid uterus profile of Figure 2.

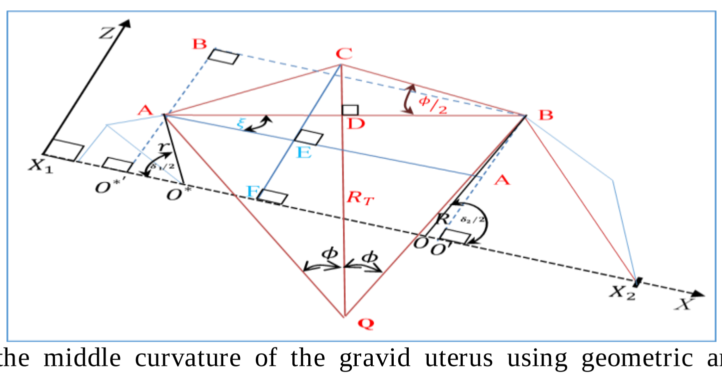

Figure 2: Estimating the middle curvature of the gravid uterus using geometric analysis; with L as the gestational fundal height, r and R are the minor and major radii of curvature at the respective wrapping angles δ_1 *and* δ_2.

ISSN: 2408-7920

African Journal of Applied Research
Vol. 5, No. 1 (2019), pp. 46-59
http://www.ajaronline.com
http://doi.org/10.26437/ajar.05.01.2019.04

The developed biomechanical model of the uterus required the generation of the 2D profile of the uterus in Matlab using Equations 10, 11 and 12. The coordinate points of the 2D profile was then obtained from Matlab (Appendix A) and used to generate the geometry using Solidworks 2016 version.

$$f(x,z) = (X^T, Z^T) \quad \text{………………………………………………………..…...…(10)}$$

$$X^T = \begin{pmatrix} x_1 \\ x_2 \\ x_3 \end{pmatrix} = \begin{pmatrix} 1 & 0 & 0 \\ 0 & 1 & 0 \\ 0 & 0 & 1 \end{pmatrix} \begin{pmatrix} r - r\cos\left(\frac{\delta 1}{2}\right) \\ L - (R + r) + r\cos\left(\frac{\delta 1}{2}\right) + \left|R\cos\left(\frac{\delta 2}{2}\right)\right| \\ R - \left|R\cos\left(\frac{\delta 2}{2}\right)\right| \end{pmatrix} \quad \text{…………...…. (11)}$$

$$Z^T = \begin{pmatrix} z_1 \\ z_2 \\ z_3 \end{pmatrix} = \begin{pmatrix} 1 & 0 & 0 \\ 0 & 1 & 0 \\ 0 & 0 & 1 \end{pmatrix} \begin{pmatrix} r\sin\left(\frac{\delta 1}{2}\right) \\ r\sin\left(\frac{\delta 1}{2}\right) + \frac{(r+R)\sin(\phi).\sin\left(\frac{\phi}{2}+\xi\right)}{\cos\left(\frac{\phi}{2}\right)} \\ \left|R\sin\left(\frac{\delta 2}{2}\right)\right| \end{pmatrix} \quad \text{…………...…...…. (12)}$$

Simulation of the Gravid Human Uterus

The cervix (tip of previa) compartment was manually generated in order to obtain a closed 2D profile of the gravid uterus. The profile was then offset to halfway in-and-out to obtain the desired thickness of 5.2 mm whilst the foetus and ligaments were manually generated using similar commands to arrive at the 2D model shown in Figure 3. It was then revolved to obtain the solid 3D model of the gravid uterus as shown in Figure 4(a). The 3D model of the gravid uterus was then imported into ANSYS for subsequent numerical analysis. A number of analysis were performed on the model using the necessary boundary equations and material properties. The ligament, uterus and foetus components were modelled as Neo Hookean material having elastic moduli versus densities of 187,000 Pa versus 1140 kg/m^3, 156,000 Pa versus 950 kg/m^3 and 24,000 versus 760 kg/m^3 respectively. Whilst the amniotic fluid was assigned a viscosity of 1.17 mPas at density of 1012.50 kg/m^3. The model was reasonably meshed *(Figure 4b & 4c)* to ensure more stable and reliable results output. The FEA Modal analysis was performed on the model using ANSYS workbench.

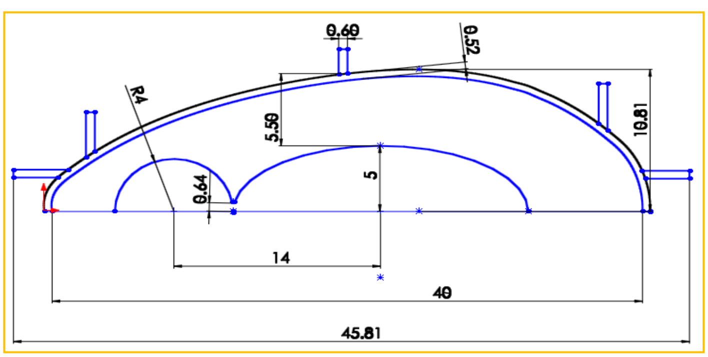

Figure 3: Manipulated Half 2D profile of gravid uterus, foetus, liquor and ligaments.

ISSN: 2408-7920

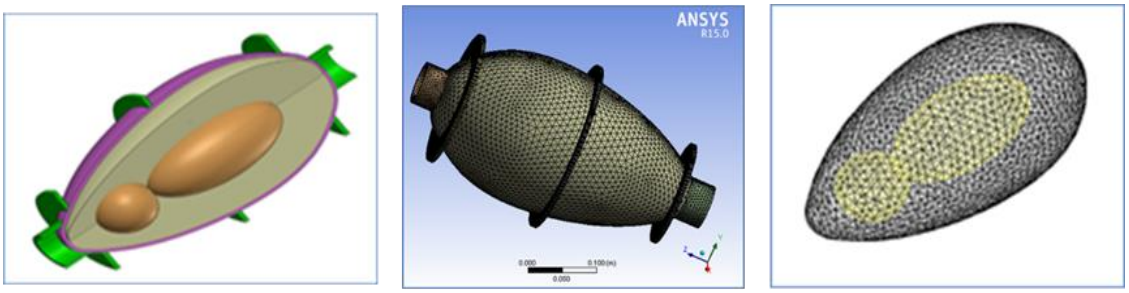

(a) (b) (c)

Figure 4: 3D model of gravid uterus and ligaments attachments and meshes of the gravid uterus model parts; (a) cut-away view (b)full mesh of gravid uterus (c) meshed liquor

3.0 DISCUSSION OF RESULTS

The results of modal analysis are captured in Figures 5 to 7 for the selective 300 mode shapes within the natural frequencies ranges of 0 – 7.25 Hz. The deformation patterns changed gradually from the lower single-digit modes of 1 - 9 to intermediate double-digit modes of 10 - 90 and finally to the higher triple-digit modes of 100 - 300. Figure 5 depict the foetal body motions and phantom deformations seen in the head, neck, thoracic, abdominal and tail compartments of the foetus at the respective natural frequencies. The deformations observed in the foetal natural shape analysis are attributed to forces generated by the vibrating liquor that engulfs the foetus.

Mode shapes 1 - 9 depict linear oscillation, angular and torsional vibratory motion of foetus about different locations of foetal body in the, z-axis, xy, xz and yz planes due to non-uniform lateral loadings in respective planes. For instance, mode shapes 4 and 5 respectively depict pure rigid body rotary vibration of the foetus about the z-direction and linear oscillatory motions of a rigid foetus along the same z-direction. Whilst mode shape 9, the most critical mode, represents an independent and opposing torsional vibrations of the head and trunk of foetus about the z-axis while the neck is fixed at a natural frequency of 1.03 Hz. The natural modes 10 to 50 represent a combination of torsional about z-axis and bending in xy, yz and xz planes of the foetal about respective perpendicular axis within frequency range of 1.39 Hz to 3.46 Hz. Particularly, mode shapes 40, 45 and 50 respectively represent completely-reversed bending loading of foetus in x and y directions. Similar deformation patterns portrayed in natural modes 60, 70, 80, 90, 100 and 150 yielded significant swelling deformations within the natural frequency range of 3.76 Hz – 5.40 Hz and realized compressive bending deformations owing to completely-reversed longitudinal and transverse loadings on foetus at varying natural frequencies. Finally, mode shapes 200 to 300 represent foetal natural deformations that resembles crooked oval deformations as though the foetus is under combined longitudinal and lateral loadings at natural frequency range of 6.06 Hz – 7.25 Hz. Moreover, in Figure 6, some detailed deformation pattern of ligaments, uterus wall, liquor and floating foetus for selected modes 60 to 150 are captured for proper comprehension.

ISSN: 2408-7920

African Journal of Applied Research
Vol. 5, No. 1 (2019), pp. 46-59
http://www.ajaronline.com
http://doi.org/10.26437/ajar.05.01.2019.04

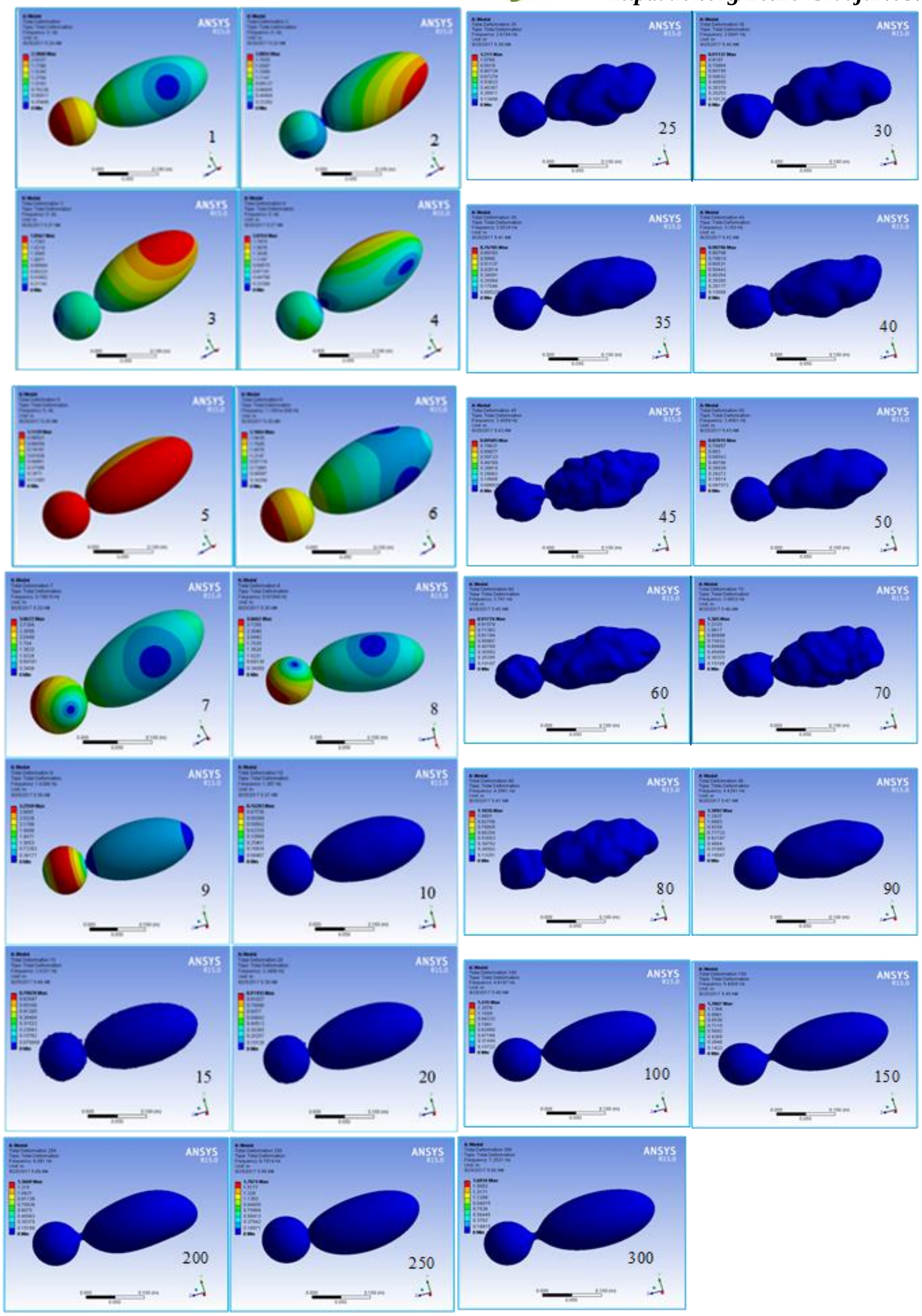

Figure 5: Mode shapes of foetus for modes 1-10; 15-50; 60-100 and mode 150-300.

ISSN: 2408-7920

Arca Academic Publisher

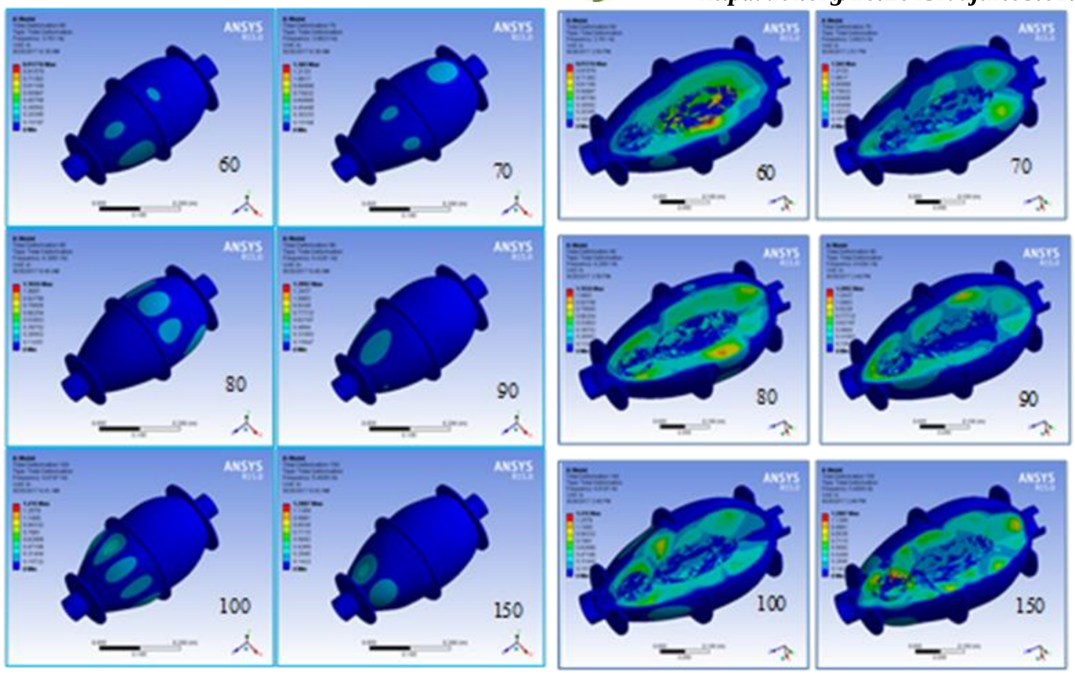

(a) *(b)*

Figure 6: Gravid human uterus modes 60 to 150 (a) and cut-away views(b)

The mode shapes of the uterus are shown in Figure 7. For mode shapes 1 – 9, inconspicuous breathing deformations were observed in the fundus, body and previa compartments of the uterus at the indicated natural frequency values. Modes 1 to 9 depict the lowest inconspicuous breathing deformation of the uterus wall due to the foetal displacement along z direction, angular deformation of foetus in xy, xz and yz planes excited the liquor molecules in the uterus and led to breathing of the uterus wall. This induced relatively lower outward pressure on the uterus and hence a subsequent bulging out of the uterus within natural frequency range of 0.00 - 1.03 Hz. Mode shapes 10 – 40 depict a mild to moderate conspicuous breathing of the uterus wall due to combined torsional and bending loadings of foetus in xy, yz and xz planes. These foetal distress and or wrinkling deformations were caused by continuous expansion and shrinkage of the main body of the uterus which translated into liquor pressure differences within the frequency range of 1.39 Hz to 3.19 Hz. The deformations experienced on the uterus walls were mostly symmetric swellings towards the previa and or fundus of the uterus. For instance, mode 35 portrays two inward and two outward oval distortions that alternate around the previa portions of the uterus whilst mode 40 has distended eight oval distortions symmetrically distributed in the previa and fundus portions of the uterus wall. Moreover, the mode shapes 45 to 100 show conspicuously high breathing deformations of the uterus wall within an increasing natural frequency range of 3.41Hz to 4.62 Hz. Mode shapes 150 to 300 exhibited uniformly high breathing deformation of the uterus wall within frequency range of 5.40 Hz to 7.25 Hz. All the uterus wall deformations witnessed in these simulations exhibited symmetric distribution of differentiated forms of the wrinkling about the cephalic axis of the uterus and foetus.

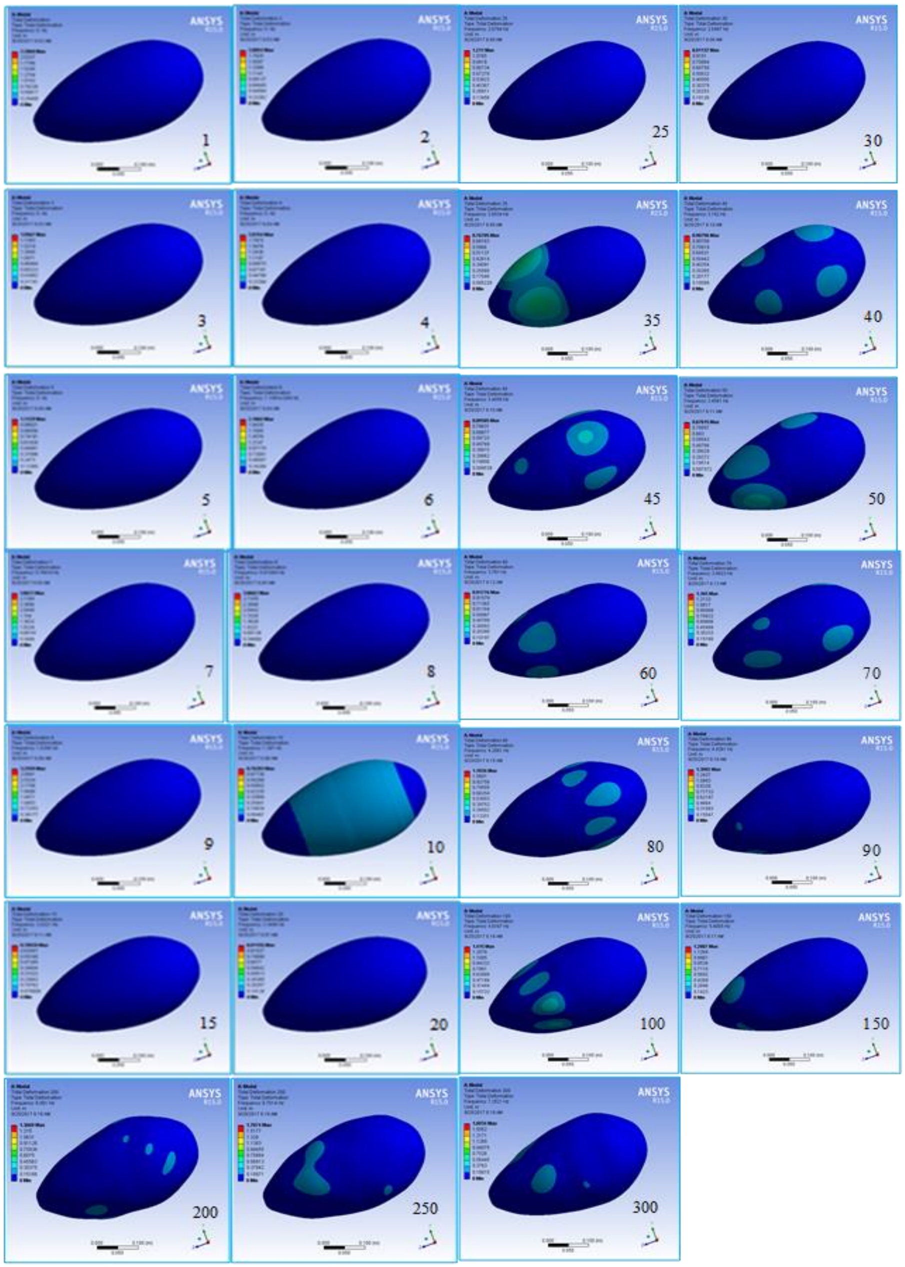

Figure 7: Mode shapes of uterus wall for modes 1-10; 15-50; 60-100 and mode 150-300.

Figure 8 depicts the natural frequencies range of 0.00 Hz -7.25 Hz versus deformations of the 300 modes of natural deformation analysis performed on the gravid human uterus. It is evident that, the different resonance frequencies of the foetus, uterus wall and the entire gravid uterus occurred at different deformation magnitudes. The ninth mode at 1.03 Hz corresponded to the principal resonance frequency of foetus with a maximum deformation of 3.26 m. This consisted of opposing torsional vibration motion of head and trunk of foetus. The uterus wall yielded two

African Journal of Applied Research
Vol. 5, No. 1 (2019), pp. 46-59
http://www.ajaronline.com
http://doi.org/10.26437/ajar.05.01.2019.04

principal resonance frequencies at 3.05 Hz and 4.62 Hz -corresponding to the 35th mode and 100th modes respectively. Meanwhile, the first three principal frequencies of the entire gravid human uterus including the foetus, uterus wall, amniotic fluid and ligaments were found to be 1.03 Hz at the ninth mode, 2.68 Hz at the 25th mode and 3.99 Hz at the 70th mode. The 1.03 Hz - 4.62 Hz range of resonance frequencies of the gravid human uterus are within the range of resonance frequency for human organs and related to human discomforts as reported by Qui and Griffin (2010), in which the seated human body has a first natural frequency between 4-5 Hz whilst those between 5-6 Hz are troublesome for the stomach.

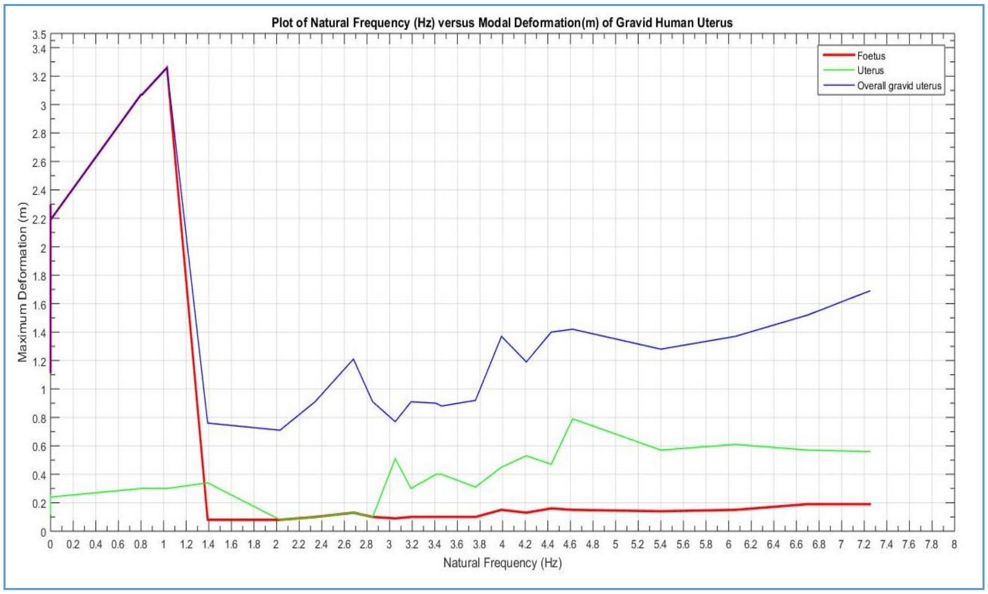

Figure 8: Natural frequency versus maximum deformation for gravid uterus.

4.0 CONCLUSION AND RECOMMENDATION

Conclusion

A biomechanical model of the gravid uterus, foetus and ligaments of a pregnant occupant exposed to ramp-induced vibrations has been developed. A total of 300 modes were examined for gravid human uterus below 7.30 Hz and mode shapes mimic the true behaviour of the gravid uterus. The modal analysis performed on the 3-dimensional model revealed that the average pregnant woman's uterus has first, second and third principal resonance in the neighbourhood of 1.03 Hz, 2.68 Hz and 3.99 Hz respectively under the plausibly postulated conditions of the human uterus compartments. These natural frequencies were mainly attributed to the severe torsional, completely-reversed longitudinal and transverse loadings on the uterus and its contents. Even though it is difficult to experimentally verify these results with analogous experimental modal analysis setup, the findings were comparable to previous works on dangerous frequency range for human beings and human organs. In surmising, this model depicts a plausible natural deformation pattern of the gravid human uterus and its foetus.

Contributions to Knowledge and Future Applications

The linear and pitch motion equations for the uterus and foetus have been developed under the stated assumptions. These equations could be used by future biomechanical engineers and health practitioners in assessing the magnitudes of linear and angular accelerations of foetus during foetal movement studies, so that in-vivo monitoring of foetal distress levels could be performed.

Moreover, the anatomical descriptions of the uterus given by researchers (*Reynolds, 1949; Sfakiani et al., 2008; Celeste & Mercer, 2008; Miftahof and Nam, 2011*;) are too theoretical and difficult to picture the geometric shape of such a gravid uterus let alone to analysis its behaviour. The developed gravid uterus equation in this work gives a more concrete, comprehensible and flexible geometric description of the gravid uterus at all gestational ages. It could be used by biomechanical engineers, gynecologists and others health practitioners for childbirth simulations, and risk assessments of the uterus during oligohydramnios and polyhydramnios conditions of pregnancy. Finally, the established natural frequencies of the uterus, foetus and ligaments serve as blueprints and foundation for future pregnancy-related biomechanical works on the uterus.

Recommendations

It is recommended that approximation of stresses and strains on the gravid human uterus under ramp-induced vibration (RIV) is crucial for future female reproductive health studies. It is also suggested that future vehicle occupant environment of new car models could be isolated from these natural frequencies to ensure absolute safety of the gravid human uterus.

REFERENCES

Ackermann, U., & Gauwerky, J., F. H. (2003). *Uterus myomatosus*. Berlin: Springer-Verlag Berlin Heidelberg.

Adama van Scheltema, P., N., In’t Anker, P., S., Vereecken, A., Vandenbussche, F., P., Kanhai, H., H., & Devlieger, R. (2005). Biochemical composition of amniotic fluid in pregnancies complicated with twin-twin transfusion syndrome. *National Center for Biotechnology Information*, *20*(3), 186–189.

Azizan, A. & Ittianuwat, R. (2016). Effect of Vibration on Occupant Driving Performances: Measured by Simulated Driving. International Journal of Scientific & Technology Research, Vol 5(1). ISSN 2277-8616.

Celeste, P. & Mercer, B. (2008). Myometerial thickness according to uterine site, gestational age and prior cesarean delivery. J Maternal Fetal Neonatal Med. 21(4): 247-250

Chheliya, N.D. (2015), mathematical modelling of viscoelastic material in active vibration control, Ganpat university, Mensana (assessed. 28/05/18)

Cho, Y., & Yoon, Y. S. (2001). Biomechanical model of human on seat with backrest for evaluating ride quality. International Journal of Industrial Ergonomics, 27(5), 331-345.

Conza, N. E. & Rixen, D. J. (2006). Experimental modal analysis on a human specimen: lessons learned. Experimental Techniques, 30(6), 51-55.

Dariusz, W., & Jaskiewicz, M. (2014). Pregnant Women When Riding in a Motor Car - Selected Issues. *Scientific Journal*, *39*(111), 169-174. Retrieved 01 26, 2018, from[http://repository.am.szczecin.pl/bitstream/handle/123456789/657/029_ZN_AM_39(111)_Wieckowski_Jaskiewicz_do_druku.pdf?sequence=1]

Fischer, R., L. (2008). Amniotic Fluid: Physiology and Assessment. http://doi.org/10.3843/GLOWM.10208

Fritsch, H., Lienemann, A., Brenner, E., & Ludwikowski, B. (2012). Clinical Anatomy of the pelvic floor. Clinical Anatomy of the pelvic floor (175). Springer Science & Business Media.

Greco, R. & Marano, G. C. (2015). Identification of parameters of Maxwell and Kelvin Voigt generalized model for fluid viscous dumpers. Journal of vibration and control, 21 (2) 260-274. Doi:10.1177/10775463134877937.

Harris, C., & Piersol, A. G. (2001). Shock and Vibration Handbook (New York (NY), US.

Kent, L. (2005). *ANSYS Workbench Tutorial*. Schroff: Development Corporation.

Klinich, K. D., Schneider, L. W., Eby, B., Rupp, J., & Pearlman, M. D. (2004). Protecting the Pregnant Occupant and the Foetus in Motor Vehicle Crahes: Biomechanical Perspective. In K. Naomi (Ed.), *Research on Women's Issues in Transportation. 2*, 135-140. Chicago: Transportation Research Board of the National Academies.

Kim, T. H., Kim, Y. T., & Yoon, Y. S. (2005). Development of a biomechanical model of the human body in a sitting posture with vibration transmissibility in the vertical direction. International Journal of Industrial Ergonomics, 35(9), 817-829.

Kitazaki, S., & Griffin, M. J. (1997). A modal analysis of whole-body vertical vibration, using a finite element model of the human body. Journal of sound and vibration, 200(1), 83-103.

Lui, H., Gao, H., & Li, P. (2013). *Handbook of Vehicle Suspension Control Systems*. The Institution of Engineering and Technology.

Matsumoto, Y., & Griffin, M. J. (2001). Modelling the dynamic mechanisms associated with the principal resonance of the seated human body. Clinical Biomechanics, 16, S31-S44.

Miftahof, R., N., & Nam, H., G. (2011). *Biomechanics of the Gravid Human Uterus* (1st ed.). Berlin and New York: Springer-Verlag Berlin Heidelberg. Retrieved from www.springer.com.

Pearlman, M. D. (2000). A comprehensive Program to Improve Safety for Pregnant Women and Foetuses in Motor Vehicle Crashes: A Preliminary Report. *American Journal of Obstetrics and Gynecology, 182*, 1554-1564.

Petyt, M. (2005). *Introduction to Finite Element Vibration Analysis*. Boca Raton, FL: CRC Press.

Qui, Y. and Griffin, M. S. (2010). Biodynamic responses of the seated human body to single - axis and dual-axis vibration. Industrial Health 48(5): 615-627.

Reynolds, S. R. (1949). Physiology of the Uterus.

Rosati, P., Pola, P., Riccardi, P., Flore, R., Tondi, P., & Bellati, U. (1991). The use of amniotic fluid viscosity measurements to establish fetal lung maturity. *International journal of Gynaecology and Obstetrics, 35*(4), 351-5. Retrieved 12 14, 2018, from [http://www.ncbi.nlm.nih.gov/pubmed/1682185]

Rubin, S. (2002). Concepts in shocks data analysis. *In: Harris. Shock and vibration handbook*. New York. New York McGrew Hill, ISBN 001137 0811.

Sfakiani, A, Buhimschi, I, Pettker, C, Magliore, L, Turan, O, Hamer, B, Buhimschi, C. (2008). Ultrasonographic evaluation of myometerial thickness in twin pregnancies. Am J Obstet Gynecol 198(5): 53, e1-10

Stolarski, T., Nakasone, Y., & Yoshimoto, S. (2007). *Engineering Analysis with ANSYS Software*.

Underwood, M., A., Gilbert, W., M., & Sherman, M., P. (2005). Amniotic Fluid: Not Just Fetal Urine Anymore. *Journal of Perinatology*, *25*, 3411–348. http://doi.org/10.1038/sj.jp.7211290

APPENDIX A: 4TH DEGREE POLYNOMIAL EQUATION FOR THE UTERUS PROFILE

```
function gravid_uterus_profile_generationn
x=[0:410.4/10000:410.4];
z = (x - 1.7e+02)/1.1e+02
y = - 3.5*z.^4 - 1.3*z.^3 - 15*z.^2 + 19*z + 76
plot(x,y)
xlabel('longitudinal profile dimensions of gravid uterus (mm)')
ylabel('transverse profile dimensions of gravid uterus (mm)')
title('Half 2D profile of gravid uterus')
A=[x' y'] ;
display(A);
```

ISSN: 2408-7920